PERGAMON

Journal of Structural Geology 23 (2001) 601–608

JOURNAL OF STRUCTURAL GEOLOGY

www.elsevier.nl/locate/jstrugeo

Effects of object ellipticity on strain, and implications for clast–matrix rocks

Susan H. Treagus*, Jack E. Treagus

Department of Earth Sciences, University of Manchester, Manchester M13 9PL, UK

Received 22 March 2000; revised 30 July 2000; accepted 8 August 2000

Abstract

We examine the influence of object shape on strain, taking the example of an elliptical object in a matrix of different viscosity. The Eshelby–Bilby equation for the cross-sectional strain of circular cylindrical objects in a matrix of different viscosity is differentiated, to express the relationship of developing sectional ellipticity on incremental strain. This leads to an expression for the strain of initial elliptical objects whose axes are parallel or perpendicular to pure shearing. Graphs show that competent elliptical objects with axial ratios of $R_i = 3$ or more, will strain significantly *more* than circular objects of the same viscosity; *less* if the objects are incompetent. While the effect is likely to be insignificant for competent objects with initial ellipticity of <2, which is indicated from statistics for undeformed pebbles in conglomerates, any clast with greater ellipticity, such as $R_i = 5$ to 10, could deform significantly more than an equant clast, and thus appear to be materially less competent. These principles have implications for geological strain studies and for competence contrasts in rocks.

1. Introduction

Since the beginnings of structural geology, researchers have recognised that different rock types deform to greater or lesser extents. These rheological differences are commonly referred to as *competence contrasts*, and are considered to control the deformation variations and structures in rocks, whether layered or aggregate. We investigate an aspect of deformation variation that is relevant to deformed clast–matrix rocks with competence contrasts, such as conglomerates. Gay (1968a,b) presented the first comprehensive modelling of these kinds of rocks, by investigating the deformation of a single isolated spherical or circular object in a matrix of different viscosity. Eshelby (1957), Gay (1968a) and Bilby et al. (1975) presented theoretical analyses to show that isolated circular-sectioned objects in an infinite matrix of contrasting properties will deform by a strain that is not equal to the far-field strain. This has important applications for rocks such as conglomerates, as the theory provides a possible means of determining viscosity ratios among different rock types (Gay, 1968b; Gay and Fripp, 1976; Lisle et al., 1983).

The deformation of non-elliptical objects in a matrix has been recently investigated by Treagus et al. (1996) and Treagus and Lan (2000), using two-dimensional finite-element analysis of variably oriented square objects in a contrasting viscous matrix. This work revealed the important difference between elliptical and non-elliptical objects. Elliptical objects deform homogeneously, maintaining elliptical forms, despite the strongly heterogenous matrix strain surrounding objects with a high viscosity contrast (Shimamoto, 1975). However, non-elliptical objects, especially angular objects of various kinds, generally deform inhomogeneously into irregular shapes according to viscosity contrast and orientation. For example, square competent objects parallel to pure shearing deform to barrel shapes, undergoing a greater overall strain than an equivalent circular object (Treagus and Lan, 2000).

What may be less obvious from object–matrix theory for circular to elliptical objects, cited above, are the interrelationships of object strain and ellipticity: the purpose of this contribution. We will concentrate on single objects in a matrix, in a two-dimensional analysis, but the findings are likely to be important to the sectional history of ellipsoidal objects in three-dimensional deformation, such as the clasts in a deforming conglomerate or diamictite.

2. Pure shear of a circular object in a contrasting matrix

The Eshelby–Bilby expression for the cross-sectional

* Corresponding author.
E-mail address: streagus@fsl.ge.man.ac.uk (S. H. Treagus).

0191-8141/01/$ - see front matter
PII: S0191-8141(00)00137-1

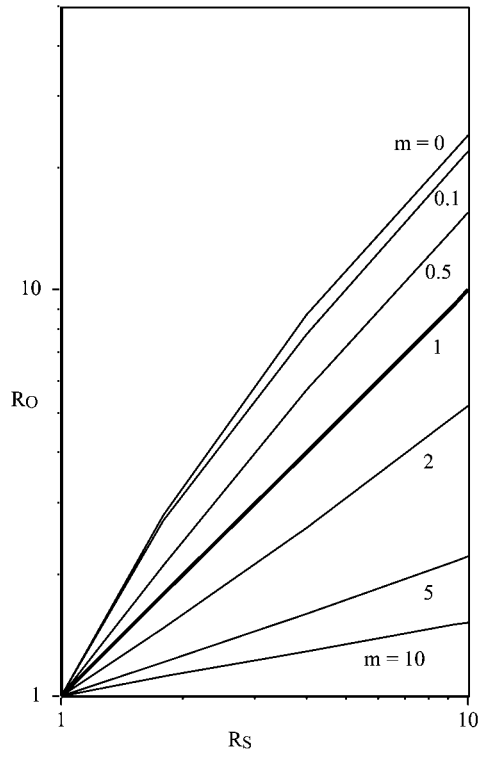

Fig. 1. Graphical representation of the Eshelby–Bilby equation (Eq. (1)), relating the strain and axial ratio (R_O) of circular to elliptical objects in a matrix, to the bulk strain ratio (R_S), on logarithmic scales. The curves show different viscosity ratios (m) of object/matrix, as numbered.

deformation of a circular cylindrical inclusion (object) in an infinite matrix, in pure shear deformation and slow incompressible viscous flow, written in familiar strain nomenclature (Bilby et al., 1975; Lisle, 1985) is:

$$\ln R_s = \ln R_o + \{(m-1)(R_o-1)/(R_o+1)\}. \quad (1)$$

The treatment is two-dimensional, and assumes adherence and continuity at the object–matrix interface. R_S is the strain ratio for the bulk far-field strain (strain ellipse axial ratio), R_O is the axial ratio of an elliptical, initially circular, object (equivalent to the object strain ratio), and m is the viscosity ratio of object to matrix (assuming Newtonian behaviour). Fig. 1 represents this equation graphically, for a range of m values, and up to bulk strain ratios of 10, which might be considered a reasonable upper limit for geological strain achieved by pure shear (i.e. <70% shortening). The curves for competent objects ($m > 1$) in Fig. 1 appear to be almost linear, although Eq. (1) is not an exact linear function of ln R_O versus ln R_S.

The expression derived by Gay (1968a) was

$$\ln R_o = \{5/(2m+3)\}\ln R_s \quad (2)$$

which is a true linear relationship of ln R_O to ln R_S. For the value ranges shown in Fig. 1, especially for competent objects ($m > 1$), this equation is found to be a good approximation to Eq. (1), but Gay's two-dimensional analysis is not considered strictly correct (see discussions: Bilby et al., 1975; Gay, 1976; Bilby et al., 1976). A linear relationship of this kind would mean that the developing object ellipticity did *not* affect the object strain path. Whether this can be assumed, absolutely or approximately, is the topic of this contribution. To answer this, it is instructive to consider Eq. (1) and its graphical representation in more detail, and over a wider range of R values than shown in Fig. 1.

Fig. 2 shows values of the Eshelby–Bilby expression (Eq. (1)) over many more orders of magnitude. It illustrates a rather narrow region of strain values for incompetent objects, between the diagonal ($m = 1$) and the limiting incompetence curve of $m = 0$, and these curves approach subparallelism to the diagonal at high R_O. In contrast, the competent ($m > 1$) object strains occupy the complete range from the graph diagonal to the abcissa which represents zero strain and thus pseudo-rigidity (here for $m \geq 50$). These

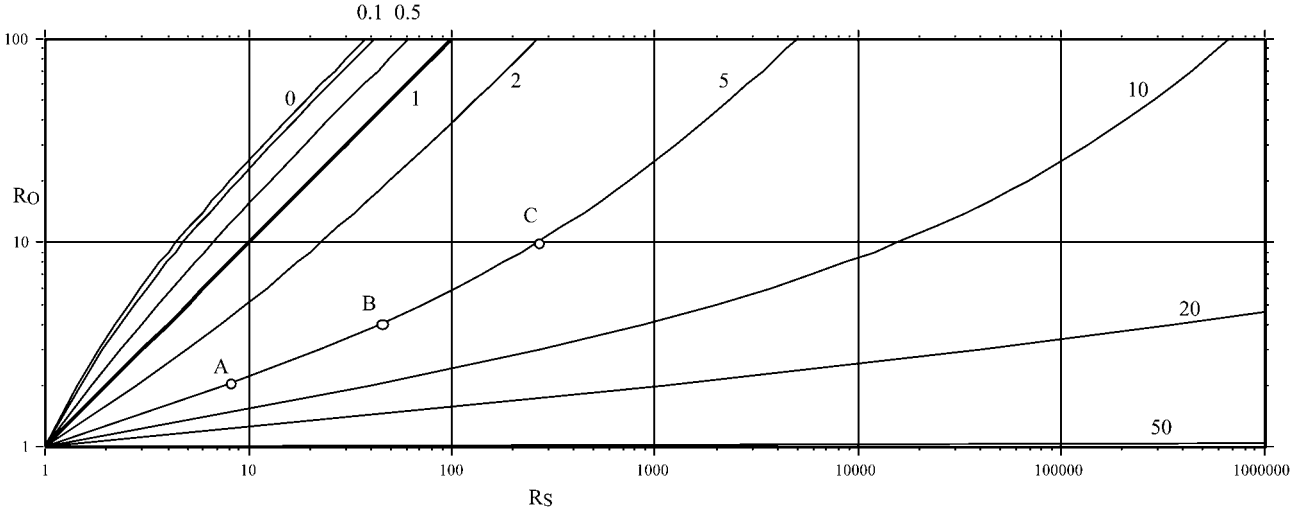

Fig. 2. Graphical representation of the Eshelby–Bilby equation (Eq. (1)), as Fig. 1, but shown over many more orders of strain magnitude. See text for further discussion, and reference to points A, B and C.

$m > 1$ curves are virtually linear from the origin up to $R_O \approx 3$, suggesting that ellipticities of < 3 have an insignificant effect on the incremental object strain. Increasing non-linearity and steepening gradients occur at higher values of R_O, and are especially notable in Fig. 2 for $m = 5$ and 10, recording the role that increasing ellipticity has on object strain. Would this effect be seen for $m = 20$ and 50, if even more cycles of bulk strain were shown? (Disregard, for the present, what the meaning is of such enormous 'strains'.) The answer is yes, but rather than demonstrate it by even wider graphs, it is better shown by defining the gradient functions for the different m curves.

2.1. Gradient function, F

The gradients of curves of ln R_O versus ln R_S graphs (e.g. Fig. 1) are given by differentiation of Eq. (1) with respect to ln R_O:

$$d(\ln R_O) = d(\ln R_S)\{(R_O + 1)^2/(R_O^2 + 2mR_O + 1)\}. \quad (3)$$

Denoting the gradient function, d(ln R_O)/d(ln R_S), as F, we have:

$$F = (R_O + 1)^2/(R_O^2 + 2mR_O + 1). \quad (4)$$

Note that this is a function of *two variables*: the viscosity ratio, m, and the instantaneous object axial ratio, R_O. When values of R_O are substituted, this reduces to a function of m, expressing the gradients of curves in Fig. 1, where they cross a particular R_O parallel.

For example, at the origin of Figs. 1 and 2, $R_O = 1$, and so

$$F = 2/(m + 1) \quad (5)$$

leading to:

$$\ln R_O = \{2/(m + 1)\}\ln R_S. \quad (6)$$

This is the *infinitesimal* strain relationship for pure shear of circular objects (Bilby et al., 1975, eq. 19). It is a linear function for ln R, and expresses the gradients of straight lines radiating from the origin of Fig. 1 or Fig. 2, in terms of their viscosity ratio, m.

For $R_O = 5$, the F function (Eq. (4)) becomes

$$F = 3.6/(m + 2.6); \ln R_O = \{3.6/(m + 2.6)\}\ln R_S. \quad (7)$$

For $R_O = 10$, we have

$$F \cong 6/(m + 5); \ln R_O \cong \{6/(m + 5)\}\ln R_S. \quad (8)$$

Note that these F expressions can thus all be written in the form:

$$F = \{(1 + p)/(m + p)\} \quad (9)$$

where p might be termed a *shape variable*. In the present case, p is related to the instantaneous value of the developing ellipse axial ratio for initially circular objects, and can be expressed (from Eq. (4)):

$$p = (R_O^2 + 1)/2R_O. \quad (10)$$

The variable, p, is found in related work to be a useful 'shape variable' for other object shapes, such as the 'squares' modelled by Treagus and Lan (2000). Its role in the rheological behaviour of object–matrix mixtures will be pursued in a fuller analysis elsewhere. Here, we are concerned only with ellipses. Using Eq. (10), it is found that $p = 1$ when $R_O = 1$ (the circular objects represented at the origin of Figs. 1 and 2). For $R_O = 5$, $p = 2.6$; for $R_O = 10$, $p \cong 5$.

This approach, in terms of F and p variables, leads us to a method of using Eq. (1) and its graphical representation (Fig. 2) for the cross-sectional deformation of *initially* elliptical cylindrical objects.

3. Pure shear of an elliptical object in a contrasting matrix

Eq. (1), after Bilby et al. (1975), is an explicit two-dimensional relationship of object and bulk strain and viscosity ratio, for pure shear of an initial circular cylindrical object. A comparable expression was not explicitly provided by these authors, for initial elliptical cylindrical objects. The deformation of elliptical objects with initial axial ratio (R_i), orientation (θ) and viscosity ratio (m), requires integration of a more complex expression (see Bilby and Kolbuszewski, 1977; Lisle et al., 1983; Lisle, 1985) that will not be given here. However, there is a way that Eq. (1) and Fig. 2 can be used, if we restrict our consideration to elliptical objects aligned parallel or perpendicular to pure shear axes.

Fig. 2 represents the progressive strain and shape change of circular objects to elliptical, in pure shear. For example, consider points A and B, on the $m = 5$ curve. At A, $R_O = 2$, and $R_S = 7.6$; at B, $R_O = 4$, and $R_S = 44.1$. Thus the *strain increment* from A to B is an object strain of $R_O = 4 \div 2 = 2$, and a bulk strain of $R_S = 44.1 \div 7.6 = 5.8$. (This can be measured additively on Fig. 2, because of its logarithmic axes.) The example demonstrates that it takes less bulk strain to achieve the second (equal) increment of object strain, than the first, as the upward-steepening $m = 5$ curve also shows. These curves can therefore also be used to track the deformation of *initial* elliptical objects with viscosity contrasts. For example, an elliptical object with $R_i = 2$ (with long axes parallel to the extension direction of pure shear), and viscosity ratio of 5, would *begin* at point A in Fig. 2, and would deform up the curve to B or C or beyond.

The theory on which Eq. (1) and Fig. 2 is based involves linear viscous incompressible fluids in slow flows. Although the matrix stress and strain states surrounding circular/elliptical objects must be inhomogeneous, because of the viscosity contrast, these objects all deform homogeneously whatever the viscosity ratio. Since there is no 'memory' involved in the deformation process, the only controls on the strain for elliptical objects aligned parallel to bulk strain axes are the ellipticity and viscosity contrast. This is also

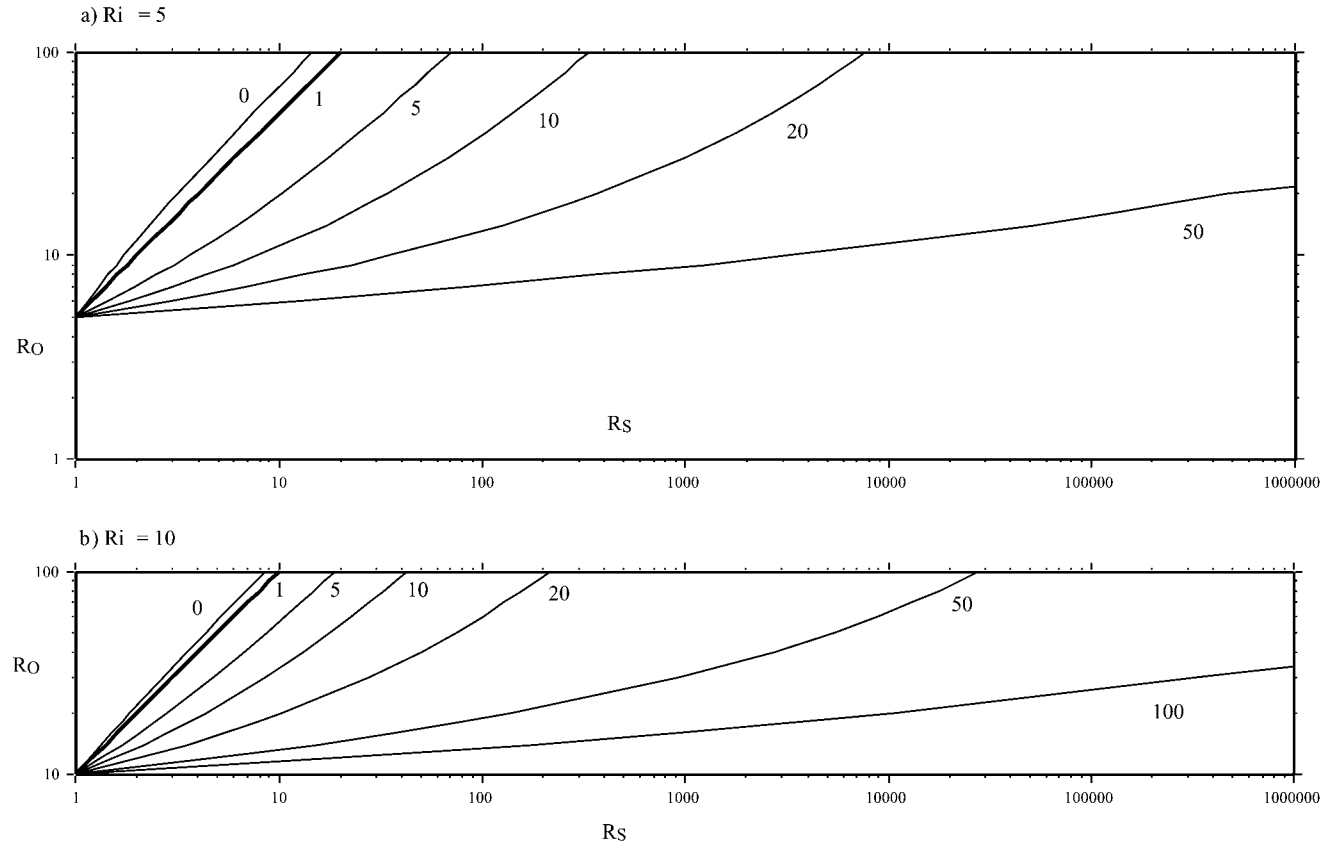

Fig. 3. Graphical representation of Eq. (13), a modification of the Eshelby–Bilby equation for the pure shear of initially elliptical objects with (a) $R_i = 5$ and (b) $R_i = 10$. Other terms and definitions as Fig. 1.

apparent from the gradient function, F (Eq. (4)). For this reason, we propose that Fig. 2 can be used with *any* R starting point to determine what happens to *any* elliptical object with its long axis parallel to pure shear extension. For example, A → B (Fig. 2) represents a change from an object with $R_i = 2$ to $R = 4$ (i.e. a true object strain of $R_O = 2$), and requires a bulk strain increment of $R_S = 5.8$. The graph is also reversible. Thus B → A can represent a 'backwards deformation' of an initial object with $R_i = 4$, which represents deformation (with $R_S = 5.8$) of an object that has its long axis *perpendicular* to pure shear extension (i.e. the object reduces its ellipticity to $R = 2$).

Fig. 2 can thus be used to compute pure shear deformation for any elliptical object that is aligned parallel/perpendicular to the strain axes. The starting points on Fig. 2 are only at the origin for initial circular objects; for any other ellipse shape we start at the appropriate ordinate R_i value on the required m-value curve. For example, for $R_i = 10$ and $m = 5$, the curve 'begins' at point C on Fig. 2. We move *up-curve* for pure shear of an object whose initial long axis is parallel to the extension; *down-curve* if the long axis is in the shortening direction. (If this is confusing, a double diagram may be used, as shown later.)

Applying this principle mathematically, we write the 'starting position' as an imaginary bulk strain, R_{S1}, after Eq. (1):

$$\ln R_{S1} = \ln R_i + \{(m-1)(R_i - 1)/(R_i + 1)\}. \quad (11)$$

A second equation expresses the 'final position' as imaginary bulk strain, R_{S2}, in terms of the final object axial ratio R_f:

$$\ln R_{S2} = \ln R_f + \{(m-1)(R_f - 1)/(R_f + 1)\}. \quad (12)$$

The *real strain* is the 'difference' between these two states: the true bulk strain, $R_S = R_{S2}/R_{S1}$, and the object strain $R_O = R_f/R_i$. From Eq. (11) and Eq. (12), we find:

$$\ln R_S = \ln R_O + (m-1)\{(R_O R_i - 1)/(R_O R_i + 1) - (R_i - 1)/(R_i + 1)\}. \quad (13)$$

This is the pure shear deformation of an initially elliptical object that is parallel or perpendicular to pure shearing.

Eq. (13) is similar to Eq. (1), but with an extra expression in curly brackets that defines initial ellipticity, R_i. ($R_i > 1$, for objects with long axes parallel to the pure shear extension; $R_i < 1$, in the perpendicular orientation.) From the earlier discussion of Fig. 2, the effect of initial ellipticity on object strain would be expected to be slight, for only moderately elliptical objects (e.g. $R_i < 3$). What happens for more

strongly elliptical objects will be examined next, using examples of $R_i = 5$ and 10.

3.1. Examples: pure shear of objects with $R_i = 5$ or 10

For elliptical objects with $R_i = 5$, Eq. (13) reduces to:

$$\ln R_S = \ln R_O + (m - 1)\{(5R_O - 1)/(5R_O + 1) - 0.67\}. \quad (14)$$

This is graphed in Fig. 3(a), and shows the slopes of different m-curves for these initial elliptical objects. Comparison with Fig. 2 shows that these $R_i = 5$ objects all deform with weaker ductility or competence contrasts than circular objects with equivalent viscosity. The effect is noticeable for the whole m range. For incompetent objects, only the $m = 0$ curve is shown, and this has moved significantly closer to the $m = 1$ diagonal, below the position for $m = 0.5$ in Fig. 2. Likewise, all the $m > 1$ curves have moved towards the diagonal, relative to Fig. 2, in positions which, for circular objects, would relate to about half these numbered viscosity ratios.

The second example shows even more elongate elliptical objects, $R_i = 10$. Eq. (13) reduces to:

$$\ln R_S = \ln R_O + (m - 1)\{(10R_O - 1)/(10R_O + 1) - 0.8\} \quad (15)$$

which is graphed in Fig. 3(b). Note the m-curves show weaker competence contrasts, again, compared to both Fig. 2 and Fig. 3(a). Even the $m = 0$ curve, that might be loosely described as a 'maximum incompetence', is only mildly different from the diagonal line, indicating *almost homogenous straining*. This is an important result, because it suggests that strongly elongate supposedly incompetent objects, whether originally elongate, or elongated through deformation, will undergo a deformation progressively approaching that of the matrix.

In rocks such as conglomerates, the clasts are usually of rocks that are considered to be more competent than the matrix and whole rock, and so examples with $m > 1$ are especially relevant. The effects shown in Fig. 3(b) for $R_i = 10$ and $m > 1$ are stronger than those shown in Fig. 3(a) for $R_i = 5$. A rough comparison with Fig. 2 shows that the m curves for $R_i = 10$ objects have approximately the same slope as those for circular objects with several factors smaller m-value. Importantly, it is demonstrated that the ellipses with viscosity ratios of 50 or 100, which if circular would be deemed 'rigid', deform as if their viscosity contrasts were considerably less. This is another important conclusion that is expected to have a bearing on how rock mixtures with strongly inequant clasts might deform.

The effect of shape on reducing the deformation and competence contrasts, as shown in Fig. 3, can be investigated another way. Referring back to Eq. (4) to (9), these express the mutual relationships among gradient, shape and viscosity. We can define m' as the viscosity ratio of circular objects (Eq. (5)) that strain on the same paths as those shown for the elliptical objects considered here ($R_i = 5$ or 10). It is found that competent objects with $R_i = 5$ have m' given by:

$$m' = (m + 0.8)/1.8 \quad (16)$$

which is almost half the real m value, as stated earlier. Competent objects with $R_i = 10$ would have m' given by:

$$m' = (m + 2)/3. \quad (17)$$

This expression again emphasises that the high m values that give rise to pseudo-rigidity in circular objects, convert to weaker competence contrasts for these high values of initial ellipticity.

It should be noted that Fig. 3 can also be produced manually from Fig. 2, by tracing all the m-curves from their $R = 5$ or 10 ordinate positions onwards (upwards) and presenting them in equivalent form (with abcissa-origin starting points). This can be done for other R values, too. However, the equations used above (Eqs. (14) and (15)) allow the curves and strains to be defined more precisely.

4. Ellipse object strain map

Rather than drawing many series of graphs of strained elliptical objects with different initial ellipticity (R_i) of the kind shown in Fig. 3, or using Fig. 2 in both 'forward' or 'backward' mode as explained earlier, which may be confusing, a special double graph can be used to illustrate the deformation of elliptical objects of a particular viscosity ratio in the two permissible orientations. Fig. 4 is an example for 'competent' elliptical objects in a matrix, with $m = 5$, and incompetent objects with $m = 0.1$. These are probably reasonable numerical values to assume for rocks (Treagus, 1999). Comparing this graph to Fig. 2, the (1, 1) point is the 'origin' for circular objects, so is marked by the circle. Elliptical objects *parallel* to the extension are shown in the upper-right graph, with the $R_i = 10$ positions shown by schematic ellipses. Elliptical objects *perpendicular* to the extension are now shown in the lower-left region, with the $R_i = 0.1$ positions shown by the ellipses on the lowest axis. The graph squares are $R = 10$ strain cycles. In this double graph, all deformation follows paths to the right and upwards. A graph on this scale is not proposed for exact calculations, but it illustrates how the gradients of strain paths for nominally competent and incompetent objects change, with initial or developing object ellipticity.

5. Ellipsoids and three dimensions

The foregoing analysis of the effect of object shape on strain has been two-dimensional, based on the theory of deformation for cross-sections of circular or elliptical cylinders in a matrix (Bilby et al., 1975). A full theoretical treatment for the pure shear deformation of spherical to ellipsoidal inclusions in a matrix of a different viscosity is

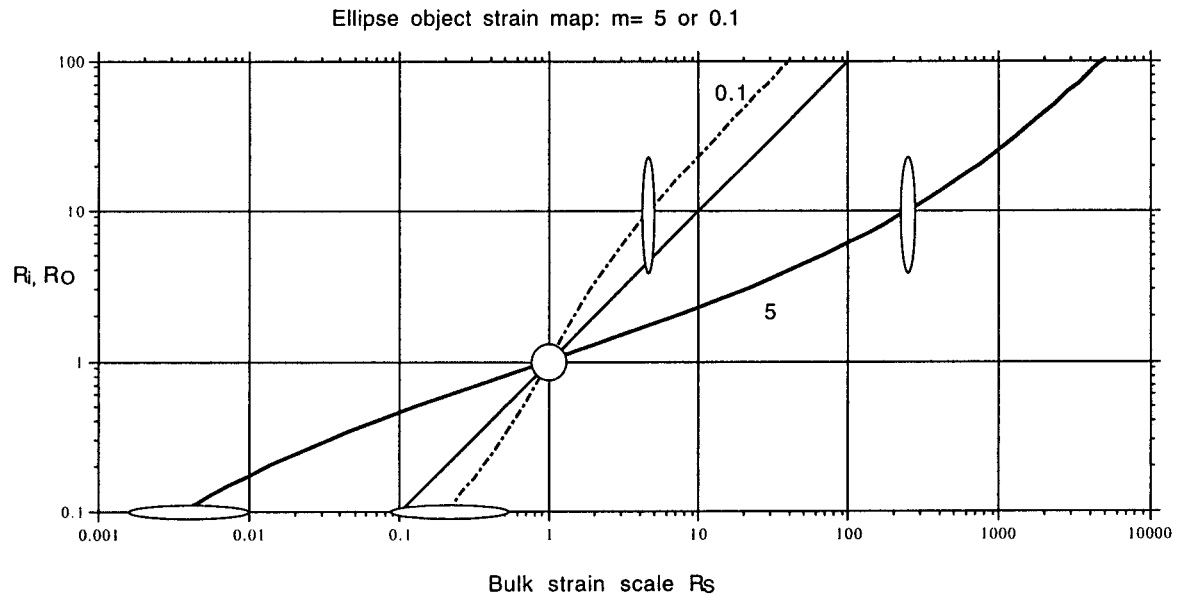

Fig. 4. Ellipse object strain map for two examples of viscosity ratio: $m = 5$ (bold curve) and 0.1 (broken curve). The diagonal shows passive behaviour ($m = 1$). The elliptical shapes ($R_O = 10$ and 0.1) are approximate representations, showing how this graph can be used to track the strain history of elliptical objects parallel or perpendicular to pure shear.

given by Freeman (1987), developed from Eshelby's (1957) equations. Significantly, Freeman demonstrated through graphical methods, including "transformed Flinn plots", that in a plane-strain pure-shear deformation, a spherical competent object would *not* deform in plane strain because of differential area strain in the principal X–Z section. The object would become prolate to some degree, depending on the viscosity contrast. Conversely, an incompetent spherical object will deform to an oblate ellipsoid. Freeman and Lisle (1987) expanded the results, and considered their applications to conglomerates and geological strain analysis.

Freeman's (1987) three-dimensional analysis depended on numerical solutions of integrals, at successive increments of deformation, and did not lead to direct algebraic solutions for object versus bulk strain, of the kind given here for two dimensions (Eq. (1)). Consequently, the differences in strain values obtained between the two-dimensional and three-dimensional analyses cannot be expressed algebraically. We have attempted a calculation from graphical information, by comparing the object and bulk strain ratios for the X-Z principal sections of object ellipsoids determined from Freeman's (1987) analysis and transformed Flinn plots ($a/b \times b/c$), with the ellipse values given by two-dimensional analysis (Fig. 1, Eq. (1)), restricting the comparison to bulk plane-strain pure shear (X/Z) of $R_S \leq 7.4$ ($\leq 63\%$ shortening). The ellipse axial-ratios for $m = 2$ to 10 are found to underestimate the ellipsoid X–Z ratio by up to 10%, but appear rather insensitive to m. For bulk strains of $R_S = 4$, the underestimate is closer to 5%. Although these values also include errors of manual measurement, we think they are small enough to justify using the two-dimensional cylinder model, and its explicit and simpler mathematics, as an approximation for the sectional deformation of spherical to ellipsoidal objects in plane strain, to geologically reasonable bulk strain values. This allows conclusions to be drawn on the effect of initial *ellipsoidal* shape on object strain. As for two dimensions, the method can only be used for ellipsoidal objects aligned with pure shear axes: in this case, the deformation of initial plane-strain ellipsoids with longest and shortest axes parallel to X or Z of pure shear, viewed in X–Z section.

6. Discussion and conclusions for rocks

We have developed a method of extending two-dimensional theory for the viscous deformation of isolated circular objects in a contrasting matrix in pure shear, to objects that were initially elliptical, with axes parallel to pure shear axes. Examples and graphs show that objects that were initially strongly elliptical deform with a smaller ductility contrast to the bulk strain than circular objects. For competent ($m > 1$) objects, this means that ellipticity increases the object's ductility, with two effects. (1) An initially elliptical object aligned in pure shearing will strain more than a circular object. At the extreme, an equant object might appear rigid and undeformed, while a strongly elliptical one of the same material could undergo measurable deformation. (2) As a competent object deforms and becomes more elliptical, it will progressively strain more, becoming increasingly ductile and apparently less competent.

For isolated incompetent ($m < 1$) objects, which by definition deform more than the bulk strain, the process works in the opposite sense: equant ones will deform the most, elongate ones the least. The range of object straining is

quite restricted, however, bounded by $m = 1$ and the 'upper' limit of $m = 0$ (Fig. 2), a maximum factor in ln$R$ of only 2. Initial or increasing ellipticity serves to narrow this range, reducing the ductility contrast to the matrix. Objects with axial ratios of 10 will behave as effectively passive strain markers, and might therefore not be interpreted as 'incompetent' at all, according to normal terms of reference.

We have argued that the two-dimensional theory, i.e. the sectional deformation of a circular/elliptical cylinder, can be extended to three dimensions, as an approximation to the plane strain deformation of a spherical/ellipsoidal object. The small amount of non-plane straining that changes competent and incompetent spherical objects into mildly prolate or oblate ellipsoids, respectively, will affect the accuracy of quantitative strain analysis, but probably by less than ±10%. We therefore consider it justified to draw some conclusions for the comparative deformation of spherical and ellipsoidal objects, viewed in the X–Z sections of plane pure shear.

The results for isolated objects in an infinite matrix might reasonably be assumed to apply to widely spaced objects, or weak suspensions of spherical/ellipsoidal objects in a matrix, such as clasts in a diamictite. Can they be applied to more closely spaced objects, such as clasts in conglomerates? In earlier discussion, Treagus et al. (1996) suggested that the finite element models of Shimamoto (1975), showing the patterns of strain in and around deformed circular objects, indicate that objects with centres spaced more than twice their diameters apart did not influence each other. This would therefore suggest that any clast–matrix mixture where the clasts have at least 'one object space' separating them may be approximated by the 'isolated object' modelling presented here, rendering it applicable to rocks with closer-spaced clasts, such as some conglomerates. We therefore follow with some discussion of deformed conglomerates, and the implications if such rocks are used in strain analysis.

If a rock contains a population of initially elongate clasts in a matrix, our analysis suggests that these should deform more uniformly with the matrix than a population of equant clasts, regardless of expected competence contrasts. For many conglomerates, the clasts will be of a rock type that is assumed to be more competent than the matrix; for example sandstone or quartzite pebbles. If these clasts have a range of initial ellipsoidal shapes, and the rock is in pure shear, the most ellipsoidal clasts with long axes parallel to the extension direction will deform the most; subspherical clasts the least.

Intriguing questions arise, therefore, when a geologist is faced with a deformed rock where some clasts are more highly elongate than others. (1) Should it be assumed that the most elongate clasts were *initially* most elongate, and that all the clasts have deformed by approximately the same strain? (2) Or have the most elongate clasts *deformed* the most, because they have a different 'competence'? The answers would not be found from clast shape and strain analysis alone, but might be indicated by the nature of deformation fabrics in the clasts and surrounding matrix. Our results suggest that both questions might be partly affirmative. The most elongate clasts in a population of competent rock-type were probably initially the most elongate, but will also have undergone the greatest strain.

This process in a population of competent clasts has the effect of widening the range of clast ellipticities with progressive deformation. In turn, this has implications for methods of geological strain analysis that often use axial ratios of competent clasts in conglomerates, such as the R_f–ϕ method (Ramsay and Huber, 1983, pp. 75–78). We have insufficient data to assess the implications of this for all the statistical methods of R_f–ϕ analysis (Lisle, 1985). Where there is a clast–matrix competence contrast, each clast can potentially deform by a different strain. An 'average clast strain' could be calculated, as for the case of passive ellipsoidal objects (Lisle, 1979; personal communication, 2000), but the data range would now contain more than mere statistical variations, so the differences among arithmetic, geometric and harmonic means, or taking square-root of $R_{f\text{-}max} \div R_{f\text{-}min}$, require theoretical assessment. However, statistics for undeformed conglomerates (Lisle, 1985, table 4.2) show that most clasts have initial ellipticities in the range of $R_i = 1.5$ to 2. If treated as competent objects, they would therefore deform only marginally more (by up to a few%) than equivalent circular objects. It might therefore be concluded that a population of mildly elliptical clasts will undergo almost uniform straining, and can therefore be analysed by R_f–ϕ methods given by Lisle (1985). However, in any statistical sample there are likely to be some clasts with much greater ellipticity, which according to our findings will have strained the most, and these would distort the statistics and perhaps lead to overestimates of average clast strain for competent objects.

Conglomerates or other rocks consisting of incompetent clasts in a competent matrix are probably rather unusual. Such a rock, if deformed, might appear almost homogeneously deformed, and thus a competence contrast between clasts and matrix might not be apparent. A clast R_f–ϕ analysis would be expected to yield a concentrated field of strain data, because any initial clast shape range will be narrowed by the process of greatest deformation of equant clasts, and least deformation of aligned elliptical clasts.

If the interrelationships of clast shape and strain for pure shear deformation, discussed here, are applicable to other deformation histories, such as simple shear, they open up the possibility of drawing wider conclusions about the deformational behaviour of clast–matrix mixtures. For example, P.D. Bons (personal communication, 2000) suggests that this may provide an explanation for the changing rheological behaviour of camphor/OCP mixtures in simple shear experiments (Bons and Urai, 1996, fig. 7). The camphor inclusions behaved as a 'hard' material, until they became more and more elongate, then apparently

yielded and behaved as layers. We aim to present a fuller investigation of the effects of clast shape on the bulk rheology of clast–matrix mixtures in a subsequent paper.

Acknowledgements

This research was supported by NERC research grant GR3/10783 (J.E.T.), and a subsequent NERC Senior Research Fellowship (S.H.T.). We appreciate receiving many constructive comments and suggestions for improvement from Richard Lisle, Dyanna Czeck, Marcia Bjornerud, Paul Bons and Richard Norris.

References

Bilby, B.A., Eshelby, J.D., Kundu, A.K., 1975. The change of shape of a viscous ellipsoidal region embedded in a slowly deforming matrix having a different viscosity. Tectonophysics 28, 265–274.

Bilby, B.A., Kolbuszewski, M.L., 1977. The finite deformation of an inhomogeneity in two-dimensional slow viscous incompressible flow. Proceedings of the Royal Society A355, 335–353.

Bilby, B.A., Eshelby, J.D., Kolbuszewski, M.L., Kundu, A.K., 1976. The change of shape of a viscous ellipsoidal region embedded in a slowly deforming matrix having a different viscosity. Some comments on a discussion by N.C. Gay. Tectonophysics 35, 408–409.

Bons, P.D., Urai, J.L., 1996. An apparatus to experimentally model the dynamics of ductile shear zones. Tectonophysics 256, 145–164.

Eshelby, J.D., 1957. The determination of the elastic field of an ellipsoidal inclusion, and related problems. Proceedings of the Royal Society A 241, 376–396.

Freeman, B., 1987. The behaviour of deformable ellipsoidal particles in three-dimensional slow flows: implications for geological strain analysis. Tectonophysics 132, 297–309.

Freeman, B., Lisle, R.J., 1987. The relationship between tectonic strain and three-dimensional shape fabrics of pebbles in deformed conglomerates. Journal of the Geological Society 144, 635–639.

Gay, N.C., 1968a. Pure shear and simple shear deformation of inhomogeneous viscous fluids. 1. Theory. Tectonophysics 5, 211–234.

Gay, N.C., 1968b. Pure shear and simple shear deformation of inhomogeneous viscous fluids. 2. The determination of the total finite strain in a rock from objects such as deformed pebbles. Tectonophysics 5, 295–302.

Gay, N.C., 1976. The change of shape of a viscous ellipsoidal region embedded in a slowly deforming matrix having a different viscosity—a discussion. Tectonophysics 35, 403–407.

Gay, N.C., Fripp, R.E.P., 1976. The control of ductility on the deformation of pebbles and conglomerates. Philosophical Transactions of the Royal Society A283, 109–128.

Lisle, R.J., 1979. Strain analysis using deformed pebbles: the influence of initial pebble shape. Tectonophysics 60, 263–277.

Lisle, R.J., 1985. Geological strain analysis. A manual for the R_f/ϕ technique. Pergamon Press, Oxford.

Lisle, R.J., Rondeel, H.E., Doorn, D., Brugge, J., van de Gaag, P., 1983. Estimation of viscosity contrast and finite strain from deformed elliptical inclusions. Journal of Structural Geology 5, 603–609.

Ramsay, J.G., Huber, M., 1983. The techniques of modern structural geology. Volume I. Strain analysis. Academic Press, London.

Shimamoto, T., 1975. The finite element analysis of the deformation of a viscous spherical body embedded in a viscous medium. Journal of the Geological Society of Japan 81, 255–267.

Treagus, S.H., 1999. Are viscosity ratios measurable from cleavage refraction? Journal of Structural Geology 21, 895–901.

Treagus, S.H., Hudleston, P.J., Lan, L., 1996. Non ellipsoidal inclusions as geological strain markers and competence indicators. Journal of Structural Geology 18, 1167–1172.

Treagus, S.H., Lan, L., 2000. Pure shear deformation of square objects, and applications to geological strain analysis. Journal of Structural Geology 22, 105–122.